

# InceptionMamba: An Efficient Hybrid Network with Large Band Convolution and Bottleneck Mamba

Yuhang Wang<sup>1</sup>, Jun Li<sup>1\*</sup>, Zhijian Wu<sup>2</sup>, Jifeng Shen<sup>3</sup>, Jianhua Xu<sup>1</sup>, Wankou Yang<sup>4</sup>

<sup>1</sup> School of Computer and Electronic Information, Nanjing Normal University, Nanjing, China

<sup>2</sup> Medical Artificial Intelligence Lab, Westlake University, Zhejiang, China

<sup>3</sup> School of Electrical and Information Engineering, Jiangsu University, Zhenjiang, China

<sup>4</sup> School of Automation, Southeast University, Nanjing, China

---

## Abstract

Within the family of convolutional neural networks, InceptionNeXt has shown excellent competitiveness in image classification and a number of downstream tasks. Built on parallel one-dimensional strip convolutions, however, it suffers from limited ability of capturing spatial dependencies along different dimensions and fails to fully explore spatial modeling in local neighborhood. Additionally, although InceptionNeXt excels at multi-scale spatial modeling capacity, convolution operations are prone to locality constraints and inherently lack the global receptive field, which is detrimental to effective global context modeling. Recent research demonstrates that Mamba based on state-space models can capture long-range dependencies while enjoying linear computational complexity. Thus, it is necessary to take advantage of the Mamba architecture to improve the long-range modeling capabilities of the InceptionNeXt while maintaining desirable efficiency. Towards this end, we propose a novel backbone architecture termed InceptionMamba in this study. More specifically, the traditional one-dimensional strip convolutions are replaced by orthogonal band convolutions in our InceptionMamba to achieve cohesive spatial modeling. Furthermore, global contextual modeling can be achieved via a bottleneck Mamba module, facilitating enhanced cross-channel information fusion and enlarged receptive field. Extensive evaluations on classification and various downstream tasks demonstrate that the proposed InceptionMamba achieves state-of-the-art performance with

---

\*Corresponding author (lijuncst@njnu.edu.cn).

superior parameter and computational efficiency. The source code will be available at <https://github.com/Wake1021/InceptionMamba>.

**Keywords:** InceptionMamba, Orthogonal Band Convolutions, Global Contextual Modeling, Bottleneck Mamba, Cross-channel Information Fusion

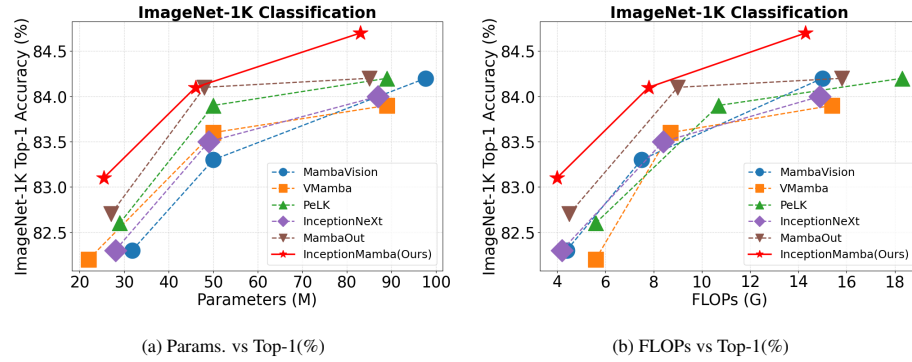


Figure 1: Performance on ImageNet-1K validation set at 224<sup>2</sup> resolutions.

## 1. Introduction

In Convolutional Neural Networks (CNNs) [1, 2, 3, 4, 5], the success of Inception architecture is largely attributed to efficient strip convolution, evolving from local feature extraction to dynamic parameter optimization [3]. Originated from InceptionNeXt [6], it is beneficial for reducing the number of parameters through asymmetric convolution decomposition (such as splitting a  $7 \times 7$  convolution into  $1 \times 7$  and  $7 \times 1$  strip convolutions). As a representative member within Inception family, InceptionNeXt has showcased the efficacy of strip convolutions in balancing computational efficiency and representational abilities. In InceptionNeXt, large-kernel depthwise convolutions are decomposed into four efficient branches including parallel one-dimensional strip convolutions, such that large-kernel CNNs are accelerated with maintained performance.

Despite achieving huge success, conventional one-dimensional strip convolutions in InceptionNeXt suffer twofold inherent limitations, which hinder their potential in complex visual understanding scenarios. On the one hand, the one-dimensional strip

convolutions are independently computed in separate channel groups, lacking sufficient spatial modeling capacity in capturing complex visual contents. For instance, while horizontal kernels effectively characterize axis-aligned patterns, their weakened responses to orthogonal structures (e.g., vertical edges) results in less discriminative encoding. Additionally, the local inductive bias of CNNs, arising from utilizing limited-size convolutional kernels (e.g.,  $3 \times 3$  convolutions) for hierarchical local feature extraction, fundamentally constrains their capacity in global contextual relationship modeling, thereby suffering from restricted receptive field. While recent efforts to addressing this limitation have explored oversized kernels [7] and dilated convolutions [8] to expand receptive fields, these approaches are challenged by accuracy-efficiency trade-off: enlarged kernels introduce a quadratic increase in computational complexity ( $O(k^2)$ ), while dilated convolutions are prone to grid artifacts that degrade spatial coherence in feature representations. In a nutshell, CNNs like InceptionNeXt with local receptive fields and weight-sharing mechanisms are highly efficient at capturing local cues but still struggle to model long-range dependencies. Consequently, it is necessary to improve the long-range modeling capacity of the InceptionNeXt while maintaining efficient parallel structure for enlarged receptive field.

Recently, a new architecture, i.e., Vision Transformer (ViT) [9, 10, 11, 12, 13, 14], has received extensive attention and emerged as a promising alternative to CNNs. ViT leverages self-attention mechanisms to enable global interactions, yet it incurs quadratic computational complexity, which poses enormous challenges to computationally intensive scenarios, e.g., dense prediction tasks. Similar to ViT, the Mamba architecture based on State Space Models has appealing long-range modeling capacity superior to CNNs. It employs a selective state transition mechanism that combines the linear complexity of convolutions with data-dependent global context modeling. Additionally, the gating mechanism allows the Mamba to dynamically focus on key spatial positions while preserving sub-quadratic computational complexity. This attribute well addresses the spatial modeling limitations of the InceptionNeXt, while hardly incurring expensive computational costs like ViT.

Taking advantage of global contextual modeling capability of Mamba, we propose an efficient hybrid backbone architecture with large band convolutions and bottleneck

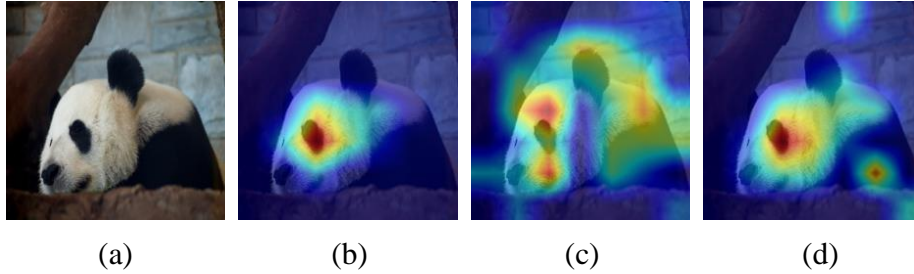


Figure 2: Visualizations of different CAMs [15] generated from ConvNeXt(b), InceptionNeXt(c) and our InceptionMamba(d) given a panda image(a). It can be observed that InceptionMamba showcases superior spatial modeling capacity in capturing semantic-aware areas in the neighborhood of panda eye and body. In contrast, InceptionNeXt only focuses on scattered eye-centric regions, yielding less cohesive representations.

Mamba termed InceptionMamba in this study. Inherited from Inception architecture, our InceptionMamba maintains Inception-style depthwise convolutions with efficient parallel structures, yet features carefully designed orthogonal band convolutions instead of the traditional one-dimensional stripe convolutions. Thus, multi-dimensional visual cues can be discovered for cohesive spatial modeling, leading to comprehensive embedding with improved representational capacity. In addition, to improve inter-channel interaction ability, we incorporate a bottleneck Mamba module into the token mixture for facilitating cross-channel information integration and enlarged receptive field. The advantages of our framework are illustrated in Fig. 2, demonstrating that InceptionMamba can capture semantically correlated local neighborhood with sufficient discriminative power. For instance, our method can accurately focus on object-aware regions surrounding panda eye and body, whereas InceptionNeXt only identify isolated eye-centric areas with degraded spatial modeling capacity.

The superiority of our InceptionMamba has been verified through extensive evaluations on various public benchmarking datasets for both classification and other downstream tasks. As shown in Fig. 1, our InceptionMamba-B attains 84.7% top-1 accuracy on ImageNet-1K, outperforming state-of-the-arts including both InceptionNeXt and Mamba-like frameworks (e.g., MambaVision [16] and VMamba [17]), while enjoying competitive computational efficiency compared to InceptionNeXt.

To summarize, our contributions in this study are fourfold as follows:

- We propose a hybrid backbone architecture termed InceptionMamba with efficient parallel structure inherited from Inception and develop a model family accordingly.
- In contrast to one-dimensional strip convolution involved in InceptionNeXt, our carefully designed orthogonal band convolutions significantly contribute to characterizing semantically cohesive visual cues in local adjacent neighborhood, thereby demonstrating improved spatial modeling capacity.
- The devised bottleneck Mamba module is conducive to inter-channel information fusion, while expanding the receptive field for enhancing global contextual modeling.
- Extensive evaluations on public benchmarking datasets for classification and other downstream tasks demonstrate that our InceptionMamba achieves state-of-the-art performance with competitive efficiency.

## 2. Related Work

### 2.1. Inception Architecture

The evolution of the Inception architecture began with the core idea of multi-scale feature fusion. Earliest Inception architecture [18, 19] introduces parallel multi-branch convolutions ( $1\times 1$ ,  $3\times 3$ ,  $5\times 5$ , and pooling) along with  $1\times 1$  dimensionality reduction to overcome the single-scale limitation. Subsequent improvements of Inception-v2 [20] and Inception-v3 [20] are manifested in enhancing computational efficiency via convolution decomposition (e.g., splitting one  $5\times 5$  convolution into two  $3\times 3$  convolutions) and batch normalization (BN). Similar pure Inception variant is Inception-v4 [21] which contains multiple consecutive Inception blocks with parallel structures. More advanced Inception-ResNet [22, 6] is a hybrid Inception network which integrates the residual learning into Inception architecture, achieving network training speedup through skip connections. A milestone work within Inception family emerges as InceptionNeXt [6] which decomposes large-kernel depthwise convolutions into multiple parallel branches of smaller kernels (e.g., square  $3\times 3$  convolutions and one-dimensional

strip convolutions), achieving desirable accuracy-throughputs trade-off in a series of downstream tasks. It is significantly beneficial for accelerating large-kernel networks with maintained performance.

## 2.2. Mamba

As a sequence modeling framework inspired by control theory, Mamba [23, 24] is a new State Space Model (SSM) which is capable of capturing long-range dependencies through the evolution of hidden states. The continuous system is defined by three core matrices: the state transition matrix  $\mathbf{A} \in \mathbb{R}^{M \times M}$ , the input projection matrix  $\mathbf{B} \in \mathbb{R}^{M \times 1}$ , and the output projection matrix  $\mathbf{C} \in \mathbb{R}^{1 \times M}$ . The system dynamics can be described as follows:

$$\begin{aligned} h'(t) &= \mathbf{A}h(t) + \mathbf{B}x(t) \\ y(t) &= \mathbf{C}h(t) \end{aligned} \tag{1}$$

To achieve efficient discrete computation, Mamba introduces zero-order preserving discretization method, which converts the continuous system into a recursive form through the time scale parameter  $\Delta$  :

$$\begin{aligned} \overline{\mathbf{A}} &= e^{\Delta \mathbf{A}} \\ \overline{\mathbf{B}} &= (\Delta \mathbf{A})^{-1} (e^{\Delta \mathbf{A}} - \mathbf{I}) \cdot \Delta \mathbf{B} \end{aligned} \tag{2}$$

Thus, the discrete state update equation is obtained:

$$\begin{aligned} h_t &= \overline{\mathbf{A}}h_{t-1} + \overline{\mathbf{B}}x_t \\ y_t &= \mathbf{C}h_t \end{aligned} \tag{3}$$

Retaining the sequence modeling characteristics of RNN, the above formulation can be reconstructed in a parallel computing manner from the global convolution perspective. The system output can be equivalently expressed as:

$$\begin{aligned} \overline{\mathbf{K}} &= (\mathbf{C}\overline{\mathbf{B}}, \mathbf{C}\overline{\mathbf{A}}\overline{\mathbf{B}}, \dots, \mathbf{C}\overline{\mathbf{A}}^{L-1}\overline{\mathbf{B}}) \\ \mathbf{y} &= \mathbf{x} * \overline{\mathbf{K}} \end{aligned} \tag{4}$$

where  $*$  represents the convolution operation, and  $\overline{\mathbf{K}} \in \mathbb{R}^L$  serves as the kernel of the SSM.

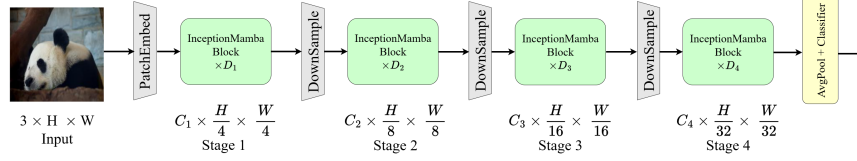


Figure 3: **Our InceptionMamba architecture with four stages.** Similar to ConvNeXt [3], InceptionMamba employs hierarchical architecture of four consecutive stages. Each stage consists of a patch embedding layer or a downsampling module, combined with  $N_i$  InceptionMamba blocks.

Recent advancements in visual Mamba models demonstrate the potential of SSM in a variety of vision tasks. In Vision Mamba [25], a bidirectional Mamba block was proposed for efficient high-resolution image processing. VMamba introduces Cross-Scan strategy to strengthen global context modeling. MambaVision combines linear complexity of Mamba with Transformer self-attention in a hybrid architecture to enhance efficiency and global spatial reasoning. Recent research explores the essence of Mamba, and reveals that Mamba is not ideally suited for all vision tasks. Meanwhile, a range of MambaOut [26] models are obtained by stacking Mamba blocks while removing their core token mixer SSM.

### 3. Method

Encouraged by recent success of vision Mamba models, we propose to deeply integrate Mamba SSM into efficient InceptionNeXt architecture with parallel structures. The former, which enjoys linear-complexity sequence modeling capability, can capture long-range spatial dependencies, whilst the latter excels at extracting key features while maintaining network efficiency. In this sense, our synergistic design helps to preserve strengths of CNNs in efficient local reasoning while enhancing model adaptability to complex scenes through global dynamic feature selection mechanism of Mamba, establishing a new foundation paradigm for a series of downstream vision tasks.

#### 3.1. Overview of InceptionMamba

Inspired by InceptionNeXt, we have designed a four-stage InceptionMamba architecture as illustrated in Fig. 3. For a given input tensor  $X \in \mathbb{R}^{B \times C \times H \times W}$  where  $B$ ,  $C$ ,

$H$ ,  $W$  represent the batch size, number of channels, height, and width, respectively, the feature processing begins with a ConvMixer module that emphasizes local spatial information encoding similar to token mixer in InceptionNeXt:

$$X' = \text{ConvMixer}(X) \quad (5)$$

The output  $X'$  is then forwarded to a Global Mixer module for global context modeling and capturing long-range dependencies:

$$X'' = \text{GlobalMixer}(X') \quad (6)$$

Then, normalization is applied to the aggregated feature expressed as:

$$Y = \text{Norm}(X'') \quad (7)$$

After normalization, the resulting feature  $Y$  is passed through a MLP module consisting of two fully connected layers, with a non-linear activation function inserted in between. These fully connected layers are typically implemented as  $1 \times 1$  convolutions for efficiency. Additionally, a residual connection is employed to facilitate gradient flow and model stability. This process is formulated as:

$$Y = \text{Conv}_{1 \times 1}^{C \rightarrow C} \{ \sigma[ \text{Conv}_{1 \times 1}^{C \rightarrow rC}(Y) ] \} + X \quad (8)$$

where  $\text{Conv}_{k \times k}^{C_i \rightarrow C_o}$  denotes a convolution operation with kernel size  $k \times k$ . Input and output channels are denoted as  $C_i$  and  $C_o$ , respectively. Additionally,  $r$  is the expansion ratio and  $\sigma$  denotes a non-linear activation function.

As the cornerstone of our method, the core InceptionMamba block constitute four-stage framework resembling ConvNeXt and InceptionNeXt, leading to a family of InceptionMamba model with varying sizes. More specifically, the block numbers in the three model variants are [3, 3, 12, 3], [4, 4, 32, 4] and [4, 4, 34, 4] for the Tiny (T), Small (S) and Base (B), respectively. Starting from an input image of  $3 \times H \times W$ , our model first applies patch embedding to process the visual data. In each stage, subsequently, downsampling operation is combined with multiple InceptionMamba blocks to progressively reduce spatial resolution, i.e., spatial size  $H \times W$  is reduced by 4 times, 16 times, 32 times, and 64 times respectively, while expanding the channel dimension

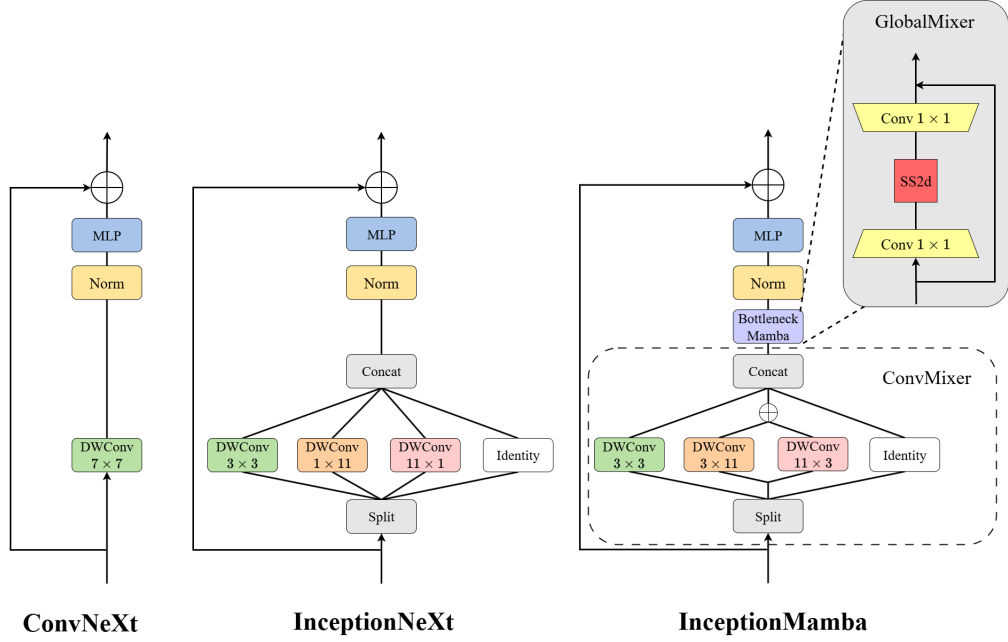


Figure 4: Illustrative comparison of ConvNeXt, InceptionNeXt, and our InceptionMamba block. InceptionMamba consists of two key components, namely ConvMixer and GlobalMixer. The former inherits efficient parallel structure from InceptionNeXt to accelerate large-kernel depthwise convolutions. Different from InceptionNeXt using one-dimensional strip convolutions, our InceptionMamba takes advantage of orthogonal band convolutions to capture multi-dimensional visual cue for cohesive feature embedding. Furthermore, the GlobalMixer adopts a carefully designed bottleneck Mamba to facilitate inter-channel information with enlarged receptive field. Compared to ConvNeXt and InceptionNeXt, our InceptionMamba enjoys efficient local spatial modeling capacity while excels in capturing long-range dependencies.

(C). This pyramid-like hierarchical architecture ends with global average pooling and classifiers for the final prediction. The architecture configurations of the three InceptionMamba variants can be referred to Table 1.

### 3.2. ConvMixer with large-kernel band convolutions

Inspired by SLaK [27] and InceptionNeXt, we devise a multi-branch structure in our ConvMixer to address the limitation of one-way large kernels. Inherited from InceptionNeXt block, the parallel structure allows speedup of large-kernel depthwise convolutions for efficient local spatial modeling. Different from its predecessor, however, our ConvMixer employs orthogonal large-kernel band convolutions instead of

Table 1: Architectures of our InceptionMamba family including Tiny (T), Small (S) and Base (B) versions.

Stage	#Tokens	Layer Specification		InceptionMamba		
				T	S	B
1	$\frac{H}{4} \times \frac{W}{4}$	PatchEmbed	Kernel Size	$3 \times 3$ , stride 2		
			Embed. Dim.	72		96
		InceptionMamba Block	Kernel size	$3 \times 3, 3 \times 11, 11 \times 3$		
			Conv. group ratio	1/8		
			Bottleneck ratio	1/2		
			MLP Ratio	4		
			# Block	3	4	
2	$\frac{H}{8} \times \frac{W}{8}$	DownSampling	Kernel Size	$3 \times 3$ , stride 2		
			Embed. Dim.	144		192
		InceptionMamba Block	Kernel size	$3 \times 3, 3 \times 11, 11 \times 3$		
			Conv. group ratio	1/8		
			Bottleneck ratio	1/2		
			MLP Ratio	4		
			# Block	3	4	
3	$\frac{H}{16} \times \frac{W}{16}$	DownSampling	Kernel Size	$3 \times 3$ , stride 2		
			Embed. Dim.	288		384
		InceptionMamba Block	Kernel size	$3 \times 3, 3 \times 11, 11 \times 3$		
			Conv. group ratio	1/8		
			Bottleneck ratio	1/2		
			MLP Ratio	4		
			# Block	12	32	34
4	$\frac{H}{32} \times \frac{W}{32}$	DownSampling	Kernel Size	$3 \times 3$ , stride 2		
			Embed. Dim.	576		768
		InceptionMamba Block	Kernel size	$3 \times 3, 3 \times 11, 11 \times 3$		
			Conv. group ratio	1/8		
			Bottleneck ratio	1/2		
			MLP Ratio	4		
			# Block	3	4	
Global average pooling, MLP						
Parameters (M)				25	46	83
FLOPs (G)				4.0	7.8	14.3

one-dimensional strip convolutions in InceptionNeXt. Band convolution can focus on larger areas with improved local modeling capability. This advantage can be intuitively shown in Fig. 2, clearly demonstrating that our InceptionMamba generates more spatially cohesive activations on the object-aware regions compared to InceptionNeXt.

Mathematically, the input features  $X$  are divided into three groups along the channel dimension via our ConvMixer as follows:

$$X_{square}, X_{band}, X_{identity} = Split(X) \quad (9)$$

which are subsequently fed into three different branches for parallel processing:

$$\begin{aligned} X_1 &= DWConv_{3 \times 3}(X_{square}) \\ X_2 &= DWConv_{3 \times 11}(X_{band}) + DWConv_{11 \times 3}(X_{band}) \\ X_3 &= X_{id} \end{aligned} \quad (10)$$

In Eq. (10), the sizes of orthogonal large-kernel band convolutions are  $3 \times 11$  and  $11 \times 3$ . Finally, the output features of each branch are concatenated as:

$$X' = Concat(X_1, X_2, X_3) \quad (11)$$

Notably, identity mapping operations are applied to the majority of channel groups in the ConvMixer while depthwise convolutions are only imposed on a small subset of groups. This is consistent with InceptionNeXt which reveals that depthwise convolutions are not required for most channels.

### 3.3. GlobalMixer with bottleneck Mamba

In the traditional InceptionNeXt architecture, the application of depthwise separable convolutions and identity mappings leads to limited channel interaction without sufficiently exploring long-range dependency. Moreover, existing deep architectures commonly suffer from redundant channel information as illustrated in Fig. 5, which inevitably increases the model complexity. To address this limitation, we design a Bottleneck Mamba structure to enhance effective cross-channel interaction and reduce channel redundancy, thereby enhancing the model capacity while hardly affecting the model efficiency. Towards this end, we design a GlobalMixer module for inter-channel

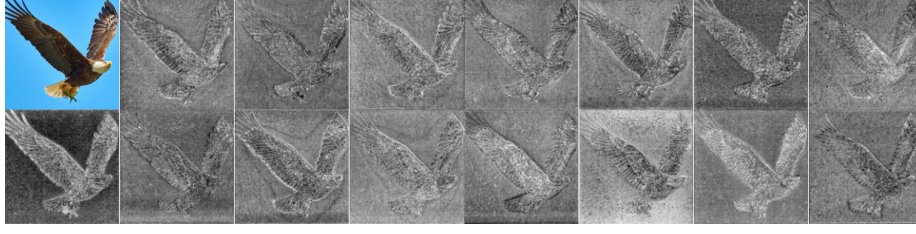


Figure 5: Visualized feature maps along consecutive channels in an intermediate layer of a pretrained VMamba model. The top-left image shows the input. Substantial redundancies in channel information can be clearly observed.

interaction at the Token layer after the ConvMixer module. Traditional methods including ConvNeXt and InceptionNeXt only pass the concatenated features through a straightforward MLP, leading to inadequate cross-channel interactions due to inherent single-channel processing characteristic of depthwise convolution. To mitigate this drawback, a bottleneck structure is introduced into the GlobalMixer, making use of  $1 \times 1$  convolution to compress and expand feature channels. This is beneficial for efficient cross-channel fusion in a low-dimensional space while retaining the key information of the original features.

To strengthen global modeling capacities while optimizing computational efficiency, a state-space module (SS2D) is integrated within the bottleneck architecture. This co-design leverages channel compression mechanism (ratio  $r = 2$ ) of the bottleneck for significantly reducing the SS2D dimensionality. More importantly, the SS2D module can capture long-range dependencies with the help of cross-scan mechanism, while the compressed feature space enjoys desirable parameter efficiency. Mathematically, given the Input  $X'$ , our GlobalMixer with a bottleneck Mamba is formulated as follows:

$$\begin{aligned}
 X'' &= \text{Conv}_{1 \times 1}^{C \rightarrow C/r}(X') \\
 X''' &= \text{SS2D}(X'') \\
 X''' &= \text{Conv}_{1 \times 1}^{C/r \rightarrow C}(X''') \\
 Y &= X + X'
 \end{aligned} \tag{12}$$

Benefiting from our efficient GlobalMixer, InceptionMamba achieves a 13.8% pa-

parameter reduction (29M→25M) and 15.2% FLOPs reduction (4.6G→4.0G) while preserving 83.1% ImageNet top-1 accuracy compared to directly utilizing SS2D for channel fusion, suggesting its potential in serving as a promising paradigm for balancing representational capacity with hardware efficiency.

### 3.4. Block Comparisons

Since our InceptionMamba is closely related to ConvNeXt and InceptionNeXt frameworks, we compare different building blocks comprising the three frameworks as illustrated in Fig. 4. With the help of the ConvMixer, our InceptionMamba block allows efficient computation of large-kernel depthwise convolutions via a parallel multi-branch structure inherited from the InceptionNeXt. Different from the predecessor which makes use of one-dimensional strip convolutions, our method features orthogonal band convolutions with improved local modeling capacity in characterizing multi-dimensional visual cues. Additionally, the GlobalMixer module with bottleneck Mamba structure can capture long-range dependencies through cross-channel interaction, which is conducive to boosting global modeling capability with expanded receptive field. In contrast, both ConvNeXt and InceptionNeXt demonstrate limited global modeling capacity, lacking GlobalMixer-like component for sufficient information fusion.

## 4. Experiments

To evaluate the proposed InceptionMamba architecture, we have carried our extensive experiments for classification and other downstream vision tasks including object detection and semantic segmentation.

### 4.1. Image classification on ImageNet

**Experimental setup.** For classification, the public ImageNet-1k [28, 29] dataset is involved in our evaluations. Our model is trained from scratch at 224×224 resolution for 300 epochs using the AdamW [30] optimizer with a weight decay of 5e-2, initial learning rate of 1e-3, and batch size of 512. The training strategy incorporates a cosine

scheduler with 10 warmup epochs, Label Smoothing of 0.1, stochastic depth, and RandAugment. For fairness, we adopt conventional data augmentation methods including Mixup, random erasing, and AutoAugment following [31]. Numerous advanced state-of-the-art backbone networks are involved in our comparative studies, including Vision-RWKV [32], Vision Mamba, Vision LSTM [33], PlainMamba [34], EfficientV-Mamba [35], VMamba, InceptionNeXt, MambaVision, QuardMamba [36], PeLK [37], MambaOut and RDNet [38]. Parallel training is performed with eight NVIDIA RTX 4090 GPUs in all our experiments.

**Results.** As shown in Table 2, our proposed InceptionMamba demonstrates consistent performance advantages across all model scales while maintaining superior computational efficiency. Among tiny models, InceptionMamba-T achieves 83.1% Top-1 accuracy with only 25.4M parameters and 4.0G FLOPs, outperforming both Mamba and CNN models like VMamba-T (82.2%) and InceptionNeXt-T (82.3%). This trend continues in small and base variants, demonstrating that InceptionMamba-S achieves 84.1% Top-1 accuracy on par with MambaOut-S with lower computational costs (7.8G vs 9.0G FLOPs). Analogously, InceptionMamba-B achieves state-of-the-art performance, reporting unrivaled 84.7% accuracy with only 83M network parameters and 14.3G FLOPs. These results validate the superiority of our InceptionMamba in accuracy-efficiency trade-off compared to existing mainstream backbone networks.

#### 4.2. Object detection & instance segmentation on COCO

**Experimental setup.** For object detection and instance segmentation, we have conducted experiments on MS-COCO [39] which contains 118k training images and 5k validation images. The detection framework is utilized as Mask R-CNN [40] with our InceptionMamba backbone, and training the detector is initialized with the model pre-trained on the ImageNet. In implementation, we follow the standard  $1\times$  training protocol (12 epochs), and adopt multi-scale data augmentation. To maintain the original aspect ratio, the input image is resized such that the shorter side is fixed at 800 pixels while the longer side does not exceed 1333 pixels. Using the AdamW optimizer, initial learning rate is set to 0.0002, whilst weight attenuation coefficient is 0.05. In comparative studies, competing architectures range from CNN and Transformer like ConvNeXt

Table 2: Performance comparison on ImageNet-1k for classification across three model scales, i.e., Tiny(T), Small(S) and Base(B).

Model	Pub.	Reso.	Params(M)	FLOPs(G)	Top-1(%)
VRWKV-S [32]	ICLR 2025	224	24	4.6	80.1
Vim-S [25]	ICML 2024	224	26	5.1	80.5
ViL-S [33]	ICLR 2025	224	23	5.1	81.5
PlainMamba-L2 [34]	BMVC 2024	224	25	8.1	81.6
EfficientVMamba-B [35]	AAAI 2025	224	33	4.0	81.8
VMamba-T [17]	NIPS 2024	224	22	5.6	82.2
InceptionNeXt-T [6]	CVPR 2024	224	28	4.2	82.3
MambaVision-T [16]	CVPR 2025	224	32	4.4	82.3
QuardMamba-S [36]	NIPS 2024	224	31	5.5	82.4
PeLK-T [37]	CVPR 2024	224	29	5.6	82.6
MambaVision-T2 [16]	CVPR 2025	224	35	5.1	82.7
MambaOut-T [26]	CVPR 2025	224	27	4.5	82.7
RDNet-T [38]	ECCV 2024	224	24	5.0	82.8
<b>InceptionMamba-T</b>	Ours	224	25	4.0	<b>83.1</b>
PlainMamba-L3 [34]	BMVC 2024	224	50	14.4	82.3
MambaVision-S [16]	CVPR 2025	224	50	7.5	83.3
InceptionNeXt-S[6]	CVPR 2024	224	49	8.4	83.5
VMamba-S [17]	NIPS 2024	224	50	8.7	83.6
RDNet-S [38]	ECCV 2024	224	50	8.7	83.7
QuardMamba-B [36]	NIPS 2024	224	50	9.3	83.8
PeLK-S [37]	CVPR 2024	224	50	10.7	83.9
MambaOut-S [26]	CVPR 2025	224	48	9.0	84.1
<b>InceptionMamba-S</b>	Ours	224	46	7.8	<b>84.1</b>
Vim-B [25]	ICML 2024	224	98	-	81.9
VRWKV-B [32]	ICLR 2025	224	94	18.2	82.0
ViL-B [33]	ICLR 2025	224	89	18.6	82.4
VMamba-B [17]	NIPS 2024	224	89	15.4	83.9
InceptionNeXt-B [6]	CVPR 2024	224	87	14.9	84.0
MambaVision-B [16]	CVPR 2025	224	98	15.0	84.2
PeLK-B [37]	CVPR 2024	224	89	18.3	84.2
MambaOut-B [26]	CVPR 2025	224	85	15.8	84.2
RDNet-B [38]	ECCV 2024	224	87	15.4	84.4
<b>InceptionMamba-B</b>	Ours	224	83	14.3	<b>84.7</b>

and Swin-Transformer to Mamba-based networks, e.g., EfficientVMamba and MambaOut.

**Results.** As illustrated in Table 3, our evaluations demonstrate superior performance of InceptionMamba across different model scales on COCO dataset. To be specific, InceptionMamba-T achieves 46.0%  $AP^b$  and 41.8%  $AP^m$  with only 43M parameters and 233G FLOPs, which consistently beats other competitors. In particular, InceptionMamba-T surpasses MambaOut-T by almost 1%  $AP^b$  with superior computational efficiency with 12.5% less FLOPs. This advantage against ConvNeXt-T is elevated to 1.8%  $AP^b$  with 10.4% less network parameters and 12.5% less FLOPs. At larger model scale, our InceptionMamba-B reports the highest 48.1%  $AP^b$  and 43.1%  $AP^m$ , which outperforms MambaOut-B and ConvNeXt-B while reducing computational costs by approximately 13% and 15%. In particular, our InceptionMamba achieves better performance than other typical Mamba-based architectures including PlainMamba, EfficientVMamba and MambaOut, sufficiently exhibiting the advantage of our framework in balancing local-aware spatial encoding and global context modeling for capturing long-range dependencies.

#### 4.3. Semantic segmentation on ADE20K

**Experimental setup.** In addition to the above-mentioned evaluations, we perform semantic segmentation experiments on public ADE20K dataset [45] using UperNet architecture [46, 47]. This dataset has 150 semantic categories with 20,000 training images and 2,000 validation images. Initialized with the pretrained model similar to the detection experiments, we follow [26] to adopt a protocol of 160,000 iterations in our training process, and utilize the AdamW optimizer with an initial learning rate set to 0.00012 and a batch size of 16.

**Results.** Table 4 presents the performance of various architectures on ADE20K dataset. It is shown that our tiny and small InceptionMamba models report respective 47.3% and 49.2% mIoU with superior efficiency, exhibiting competitive performance compared to corresponding VMamba and MambaOut competitors. When extending our framework to larger scales, the resulting InceptionMamba-B achieves 50.1% mIoU

Table 3: Performance comparison on COCO for object detection and instance segmentation. Mask R-CNN is used as detection framework.

Backbone	Params(M)	FLOPs(G)	$AP^b$	$AP^m$
ConvNeXt-T [3]	48	262	44.2	40.1
Swin-T [41]	48	267	42.7	39.3
ViT-Adapter-S [42]	48	403	44.7	39.9
PVTv2-B2 [43]	45	309	45.3	41.2
EfficientVMamba-B [35]	53	252	43.7	40.2
PlainMamba-L1 [34]	31	388	44.1	39.1
MambaOut-T [26]	43	262	45.1	41.0
<b>InceptionMamba-T</b>	43	233	<b>46.0</b>	<b>41.8</b>
ConvNeXt-S [3]	70	348	45.4	41.8
Swin-S [41]	69	354	44.8	40.9
PVTv2-B3 [43]	65	397	47.0	42.5
MambaOut-S [26]	65	354	47.4	42.7
<b>InceptionMamba-S</b>	63	301	<b>47.5</b>	<b>42.6</b>
ConvNeXt-B [3]	108	486	47.0	42.7
Swin-B [41]	107	496	46.9	42.3
ViT-Adapter-B [42]	102	557	47.0	41.8
PVTv2-B5 [43]	102	557	47.4	42.5
MambaOut-B [26]	100	495	47.4	43.0
<b>InceptionMamba-B</b>	99	421	<b>48.1</b>	<b>43.1</b>

Table 4: Comparison of semantic segmentation results on ADE20K dataset using UperNet.

Backbone	Params(M)	FLOPs(G)	mIoU(%)
ConvNeXt-T [3]	60	939	46.0
Swin-T [41]	60	945	44.4
Focal-T [44]	62	998	45.8
MambaVision-T [16]	55	945	46.0
EfficientVMamba-B [35]	65	930	46.5
VMamba-T [17]	55	964	47.3
MambaOut-T [26]	54	938	47.4
<b>InceptionMamba-T</b>	53	928	<b>47.3</b>
ConvNeXt-S [3]	82	1027	48.7
Swin-S [41]	81	1038	47.6
Focal-S [44]	85	1130	48.0
MambaVision-S [16]	84	1135	48.2
VMamba-S [17]	76	1081	49.5
MambaOut-S [26]	76	1032	49.5
<b>InceptionMamba-S</b>	73	1006	<b>49.2</b>
ConvNeXt-B [3]	122	1170	49.1
Swin-B [41]	121	1188	48.1
Focal-B [44]	126	1354	49.0
MambaVision-B [16]	126	1342	49.1
VMamba-B [17]	110	1226	50.0
MambaOut-B [26]	112	1178	49.6
<b>InceptionMamba-B</b>	110	1145	<b>50.1</b>

Table 5: Comparison Results of different settings of Branch Ratios (square conv./Band conv./Identity Mapping) within ConvMixer. The GlobalMixer is excluded from our InceptionMamba.

Branch ratio	Params(M)	FLOPs(G)	Top-1(%)
[0.125, 0.125, 0.75]	21.4	3.35	81.9
[0.125, 0.25, 0.625]	21.5	3.37	81.7
[0.25, 0.25, 0.5]	21.5	3.38	81.9

with 110M parameters and 1145G FLOPs, which outperforms all the other competing networks in both accuracy and efficiency. These comparisons further reveal the potential of our hybrid architecture in combining local-aware encoding and global context modeling.

#### 4.4. Ablation studies

**Branch ratio.** To investigate the impact of different branch allocation ratios on model performance within ConvMixer, we have conducted ablation experiments comparing three different channel allocation strategies in our model excluding GlobalMixer module. The experimental results as shown in Table 5 demonstrate that the best 81.9% Top-1 accuracy is reported when employing a ratio of [0.125, 0.125, 0.75] with 21.4M parameters and 3.35G FLOPs, exhibiting the optimal balance between accuracy and efficiency. In contrast, increasing the ratio of the second branch to 0.25 ([0.125, 0.25, 0.625]) leads to a slight parameter increase to 21.5M and a marginal performance drop (81.7%), indicating that the asymmetric convolutional branches are sensitive to channel variations. A balanced allocation scheme ([0.25, 0.25, 0.5]) maintains 81.9% accuracy with comparable computational cost (3.38G FLOPs), verifying the robustness of the module design to different allocation ratios. After comprehensive evaluation, the branch ratio is empirically set as [0.125, 0.125, 0.75] in our remaining experiments, as it achieves the best accuracy-efficiency trade-off.

**ConvMixer.** To delve into the ConvMixer within our InceptionMamba, we have conducted comprehensive ablation studies by comparing our ConvMixer with two different designs: Depthwise convolutions within ConvNeXt and decomposed convolutions

Table 6: Comparison Results of Different structures within our ConvMixer.

ConvMixer	Params(M)	FLOPs(G)	Top-1(%)
DWConv3×3	25.4	4.0	82.8
InceptionDWConv2d	25.4	4.0	82.9
Strip convolution	25.4	4.0	83.0
<b>Ours</b>	<b>25.4</b>	<b>4.0</b>	<b>83.1</b>

Table 7: Comparison of SS2D (Mamba) and Bottleneck + SS2D (GlobalMixer).

Global mixer	Params(M)	FLOPs(G)	Top-1(%)	TP.(imgs/s)
SS2D	29	4.6	83.1	1042
<b>Bottleneck + SS2D</b>	<b>26</b>	<b>4.0</b>	<b>83.1</b>	<b>1362</b>

within InceptionNeXt. We also replaced band convolution with strip convolution for comparison. As demonstrated in Table 6, our proposed ConvMixer achieves superior performance while maintaining identical model complexity.

**Necessity of Bottleneck.** Moreover, we explore the benefits of bottleneck structure within our GlobalMixer. As shown in Table 7, integrating the bottleneck with SS2D maintains model accuracy while significantly improving efficiency. Compared to the baseline SS2D, introducing the bottleneck achieves the same Top-1 accuracy while reducing both parameters and computational costs by over 10%. Additionally, the throughput increases substantially, highlighting the ability of the bottleneck in efficiently compressing feature dimensions without sacrificing model performance as aforementioned.

**GlobalMixer.** To further investigate the GlobalMixer within our framework, we have systematically evaluated different architectures involving the bottleneck as illustrated in Table 8. Compared to the baseline without Mamba Bottleneck, all the other variants involving bottleneck improve Top-1 accuracy. In particular, our GlobalMixer achieves the highest 83.1% Top-1 accuracy, while maintaining competitive efficiency by reduc-

Table 8: Comparison of different modules involving Bottleneck structure.

Global mixer	Params(M)	FLOPs(G)	Top-1(%)	TP.(imgs/s)
no Bottleneck Mamba	21.4	3.3	81.9	2255
Bottleneck + GELU	23.5	3.6	82.1	1976
Bottleneck + DWConv7×7	23.6	4.0	82.1	1880
Bottleneck + attention	26.4	4.6	82.3	1305
<b>Bottleneck + SS2D</b>	<b>25.4</b>	<b>4.0</b>	<b>83.1</b>	<b>1362</b>

ing FLOPs by 13% compared to the structure of Bottleneck + attention (LiteMLA linear attention in EfficientViT [48]) and promoting the throughput from 1305 imgs/s to 1362 imgs/s. Notably, while Bottleneck + attention slightly improves accuracy, it leads to significantly increased computational cost. This contrast suggests the advantage of SS2D in balancing between performance and efficiency. Simpler designs like Bottleneck + GELU or Bottleneck + DWConv7×7 achieve marginal performance gains but fail to rival SS2D in terms of global modeling capability. These results demonstrate that our GlobalMixer incorporating SS2D and bottleneck optimally leverages hardware-friendly operations (e.g., linear complexity scans) to achieve accuracy-speed trade-off, thereby well aligning with the efficiency goal of modern lightweight architectures.

**More Visualization Results.** To qualitatively demonstrate the advantages of the proposed InceptionMamba, we intuitively compare our method with the classic ConvNeXt and InceptionNeXt frameworks. As illustrated in Fig. 6, given an input “dog” image, InceptionMamba produces CAMs that can capture object-aware regions more comprehensively and accurately, leading to high responses to the regions of the dog’s limbs and head. In contrast, for the input “cat” image, ConvNeXt mainly focuses on the face of the cat, while InceptionNeXt pays attention to the cat’s legs area. In contrast, our InceptionMamba can capture key regions including the cat’s head and body area that are highly semantically relevant to the “cat” class. This indicates that our InceptionMamba architecture can improve global context modeling capacity while inherits multi-scale feature fusion from Inception-like structures. Besides, the qualitative comparisons demonstrate that InceptionMamba can capture richer spatial relationships, manifesting

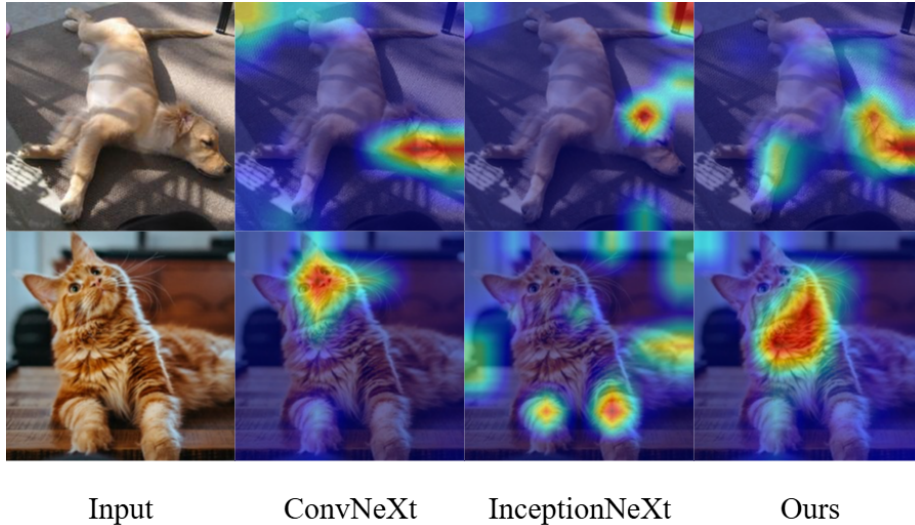


Figure 6: Comparison of CAMs generated from different mainstream architectures. Our InceptionMamba is capable of characterizing key semantic-aware regions, which is beneficial for a variety of downstream vision tasks.

itself as a potential state-of-the-art lightweight architecture. This also complements previous ablation results regarding the advantage of our method in efficiency-accuracy trade-off.

## 5. Conclusion

In this study, we propose a hybrid backbone architecture termed InceptionMamba. Inheriting efficient parallel structure from InceptionNeXt framework, we leverage large band depthwise convolutions within our ConvMixer for capturing local cues and develop bottleneck Mamba for channel interaction, such that long-range dependencies modeling capability can be significantly improved. Extensive experiments demonstrate the superiority of InceptionMamba in terms of both accuracy and computational efficiency compared to existing mainstream CNNs and ViT architectures on various public benchmarks spanning image classification and several downstream vision tasks. We hope our work can inspire the exploration of efficient multi-scale global interaction paradigms in deep architecture design and facilitate the development of lightweight yet

powerful vision backbones.

### **Acknowledgment**

This work was supported by the National Natural Science Foundation of China under Grant 62173186, 62076134, 62276061, and the Key R & D Program of Zhejiang Province (2024C04056(CSJ)).

### **References**

- [1] Y. LeCun, B. Boser, J. S. Denker, D. Henderson, R. E. Howard, W. Hubbard, L. D. Jackel, Backpropagation applied to handwritten zip code recognition, *Neural Computation* 1 (4) (1989) 541–551.
- [2] Y. LeCun, L. Bottou, Y. Bengio, P. Haffner, Gradient-based learning applied to document recognition, *Proceedings of the IEEE* 86 (11) (1998) 2278–2324.
- [3] Z. Liu, H. Mao, C.-Y. Wu, C. Feichtenhofer, T. Darrell, S. Xie, A ConvNet for the 2020s, in: *Proceedings of the IEEE/CVF Conference on Computer Vision and Pattern Recognition (CVPR)*, 2022, pp. 11966–11976.
- [4] K. He, X. Zhang, S. Ren, J. Sun, Deep residual learning for image recognition, in: *Proceedings of the IEEE/CVF Conference on Computer Vision and Pattern Recognition (CVPR)*, 2016, pp. 770–778.
- [5] G. Huang, Z. Liu, L. van der Maaten, K. Q. Weinberger, Densely connected convolutional networks, in: *Proceedings of the IEEE Conference on Computer Vision and Pattern Recognition (CVPR)*, 2017, pp. 2261–2269.
- [6] W. Yu, P. Zhou, S. Yan, X. Wang, Inceptionnext: When inception meets convnext, in: *Proceedings of the IEEE/CVF Conference on Computer Vision and Pattern Recognition (CVPR)*, 2024, pp. 5672–5683.
- [7] X. Ding, X. Zhang, J. Han, G. Ding, Scaling up your kernels to  $31 \times 31$ : Revisiting large kernel design in CNNs, in: *Proceedings of the IEEE/CVF Conference on Computer Vision and Pattern Recognition (CVPR)*, 2022, pp. 11953–11965.

- [8] F. Yu, V. Koltun, Multi-scale context aggregation by dilated convolutions, in: Proceedings of the International Conference on Learning Representations (ICLR), 2016, pp. 1–13.
- [9] A. Dosovitskiy, L. Beyer, A. Kolesnikov, D. Weissenborn, X. Zhai, T. Unterthiner, M. Dehghani, M. Minderer, G. Heigold, S. Gelly, J. Uszkoreit, N. Houlsby, An image is worth 16x16 words: Transformers for image recognition at scale, in: Proceedings of International Conference on Learning Representations (ICLR), 2021, pp. 1–22.
- [10] I. Tolstikhin, N. Houlsby, A. Kolesnikov, L. Beyer, X. Zhai, T. Unterthiner, J. Yung, A. Steiner, D. Keysers, J. Uszkoreit, M. Lucic, A. Dosovitskiy, MLP-Mixer: An all-MLP architecture for vision, in: Advances in Neural Information Processing Systems (NeurIPS), 2021, pp. 1–12.
- [11] A. Steiner, A. Kolesnikov, , X. Zhai, R. Wightman, J. Uszkoreit, L. Beyer, How to train your ViT? data, augmentation, and regularization in Vision Transformers, arXiv preprint arXiv:2106.10270 (2021).
- [12] X. Chen, C.-J. Hsieh, B. Gong, When Vision Transformers outperform ResNets without pretraining or strong data augmentations, in: Proceedings of International Conference on Learning Representations (ICLR), 2022, pp. 1–20.
- [13] J. Zhuang, B. Gong, L. Yuan, Y. Cui, H. Adam, N. Dvornek, S. Tatikonda, J. Duncan, T. Liu, Surrogate gap minimization improves sharpness-aware training, in: Proceedings of International Conference on Learning Representations (ICLR), 2022, pp. 1–24.
- [14] X. Zhai, X. Wang, B. Mustafa, A. Steiner, D. Keysers, A. Kolesnikov, L. Beyer, LiT: Zero-shot transfer with locked-image text tuning, in: Proceedings of the IEEE/CVF Conference on Computer Vision and Pattern Recognition (CVPR), 2022, pp. 18102–18112.
- [15] R. R. Selvaraju, M. Cogswell, A. Das, R. Vedantam, D. Parikh, D. Batra, Grad-CAM: Visual explanations from deep networks via gradient-based localiza-

- tion, in: Proceedings of the IEEE International Conference on Computer Vision (ICCV), 2017, pp. 618–626.
- [16] A. Hatamizadeh, J. Kautz, Mambavision: A hybrid mamba-transformer vision backbone, in: Proceedings of the IEEE/CVF Conference on Computer Vision and Pattern Recognition (CVPR), 2025, pp. 25261–25270.
  - [17] Y. Liu, Y. Tian, Y. Zhao, H. Yu, L. Xie, Y. Wang, Q. Ye, Y. Liu, VMamba: Visual state space model, in: Advances in Neural Information Processing Systems (NeurIPS), 2024, pp. 103031–103063.
  - [18] C. Szegedy, W. Liu, Y. Jia, P. Sermanet, S. Reed, D. Anguelov, D. Erhan, V. Vanhoucke, A. Rabinovich, Going deeper with convolutions, in: Proceedings of the IEEE/CVF Conference on Computer Vision and Pattern Recognition (CVPR), 2015, pp. 1–9.
  - [19] C. Szegedy, V. Vanhoucke, S. Ioffe, J. Shlens, Z. Wojna, Rethinking the inception architecture for computer vision, in: Proceedings of the IEEE/CVF Conference on Computer Vision and Pattern Recognition (CVPR), 2016, pp. 2818–2826.
  - [20] C. Szegedy, V. Vanhoucke, S. Ioffe, J. Shlens, Z. Wojna, Rethinking the inception architecture for computer vision, in: Proceedings of the IEEE Conference on Computer Vision and Pattern Recognition (CVPR), 2016, pp. 2818–2826.
  - [21] C. Szegedy, S. Ioffe, V. Vanhoucke, A. Alemi, Inception-v4, inception-resnet and the impact of residual connections on learning, in: Proceedings of the AAAI Conference on Artificial Intelligence, 2017, pp. 4278–4284.
  - [22] X. Ding, X. Zhang, J. Han, G. Ding, Diverse branch block: Building a convolution as an inception-like unit, in: Proceedings of the IEEE/CVF Conference on Computer Vision and Pattern Recognition (CVPR), 2021, pp. 10881–10890.
  - [23] A. Gu, T. Dao, Mamba: Linear-time sequence modeling with selective state spaces, arXiv preprint arXiv:2312.00752 (2023).

- [24] T. Dao, A. Gu, Transformers are SSMS: Generalized models and efficient algorithms through structured state space duality, in: International Conference on Machine Learning (ICML), 2024, pp. 10041–10071.
- [25] L. Zhu, B. Liao, Q. Zhang, X. Wang, W. Liu, X. Wang, Vision Mamba: Efficient visual representation learning with bidirectional state space model, in: Proceedings of International Conference on Machine Learning (ICML), 2024, pp. 62429–62442.
- [26] W. Yu, X. Wang, MambaOut: Do we really need Mamba for vision?, in: Proceedings of the IEEE/CVF Conference on Computer Vision and Pattern Recognition (CVPR), 2025, pp. 4484–4496.
- [27] S. Liu, T. Chen, X. Chen, X. Chen, Q. Xiao, B. Wu, M. Pechenizkiy, D. Mocanu, Z. Wang, More convnets in the 2020s: Scaling up kernels beyond 51x51 using sparsity, in: Proceedings of International Conference on Learning Representations (ICLR), 2022, pp. 1–23.
- [28] J. Deng, W. Dong, R. Socher, L. Li, K. Li, L. Fei-Fei, Imagenet: A large-scale hierarchical image database, in: Proceedings of the IEEE/CVF Conference on Computer Vision and Pattern Recognition (CVPR), 2009, pp. 248–255.
- [29] O. Russakovsky, J. Deng, H. Su, J. Krause, S. Satheesh, S. Ma, Z. Huang, A. Karpathy, A. Khosla, M. Bernstein, et al., Imagenet large scale visual recognition challenge, International Journal of Computer Vision 115 (3) (2015) 211–252.
- [30] I. Loshchilov, F. Hutter, Decoupled weight decay regularization, in: Proceedings of International Conference on Learning Representations (ICLR), 2019, pp. 1–22.
- [31] H. He, J. Zhang, Y. Cai, H. Chen, X. Hu, Z. Gan, Y. Wang, C. Wang, Y. Wu, L. Xie, MobileMamba: Lightweight multi-receptive visual Mamba network, Proceedings of the IEEE/CVF Conference on Computer Vision and Pattern Recognition (CVPR) (2025).
- [32] Y. Duan, W. Wang, Z. Chen, X. Zhu, L. Lu, T. Lu, Y. Qiao, H. Li, J. Dai, W. Wang, Vision-RWKV: Efficient and scalable visual perception with rwkv-like architec-

- tures, in: Proceedings of International Conference on Learning Representations (ICLR), 2025, pp. 1–17.
- [33] B. Alkin, M. Beck, K. Pöppel, S. Hochreiter, J. Brandstetter, Vision-LSTM: xLSTM as generic vision backbone, in: Proceedings of International Conference on Learning Representations (ICLR), 2025, pp. 1–22.
  - [34] C. Yang, Z. Chen, M. Espinosa, L. Ericsson, Z. Wang, J. Liu, E. J. Crowley, PlainMamba: Improving non-hierarchical Mamba in visual recognition, in: Proceedings of British Machine Vision Conferenc (BMVC), 2024, pp. 1–22.
  - [35] X. Pei, T. Huang, C. Xu, EfficientVMamba: Atrous selective scan for light weight visual mamba, in: Proceedings of the AAAI Conference on Artificial Intelligence, 2025, pp. 6443–6451.
  - [36] F. Xie, W. Zhang, Z. Wang, C. Ma, QuadMamba: Learning quadtree-based selective scan for visual state space model, in: Advances in Neural Information Processing Systems (NeurIPS), 2024, pp. 117682–117707.
  - [37] H. Chen, X. Chu, Y. Ren, X. Zhao, K. Huang, PeLK: Parameter-efficient large kernel convnets with peripheral convolution, in: Proceedings of the IEEE/CVF Conference on Computer Vision and Pattern Recognition (CVPR), 2024, pp. 5557–5567.
  - [38] D. Kim, B. Heo, D. Han, DenseNets Reloaded: Paradigm shift beyond ResNets and ViTs, in: Proceedings of European Conference on Computer Vision (ECCV), 2024, pp. 395–415.
  - [39] T.-Y. Lin, M. Maire, S. Belongie, J. Hays, P. Perona, D. Ramanan, P. Dollár, C. L. Zitnick, Microsoft coco: Common objects in context, in: Proceedings of the European Conference on Computer Vision (ECCV), 2014, pp. 740–755.
  - [40] K. He, G. Gkioxari, P. Dollár, R. Girshick, Mask R-CNN, in: Proceedings of the IEEE International Conference on Computer Vision (ICCV), 2017, pp. 2961–2969.

- [41] Z. Liu, Y. Lin, Y. Cao, H. Hu, Y. Wei, Z. Zhang, S. Lin, B. Guo, Swin Transformer: Hierarchical Vision Transformer using shifted windows, in: Proceedings of the IEEE/CVF International Conference on Computer Vision (ICCV), 2021, pp. 9992–10002.
- [42] Z. Chen, Y. Duan, W. Wang, J. He, T. Lu, J. Dai, Y. Qiao, Vision transformer adapter for dense predictions, in: Proceedings of the International Conference on Learning Representations (ICLR), 2022, pp. 1–20.
- [43] W. Wang, E. Xie, X. Li, D.-P. Fan, K. Song, D. Liang, T. Lu, P. Luo, L. Shao, Pvt2: Improved baselines with pyramid vision transformer, *Computational Visual Media* 8 (3) (2022) 1–10.
- [44] J. Yang, C. Li, X. Dai, J. Gao, Focal modulation networks, in: Advances in Neural Information Processing Systems (NeurIPS), 2022, pp. 4203–4217.
- [45] B. Zhou, H. Zhao, X. Puig, S. Fidler, A. Barriuso, A. Torralba, Scene parsing through ade20k dataset, in: Proceedings of the IEEE/CVF Conference on Computer Vision and Pattern Recognition (CVPR), 2017, pp. 633–641.
- [46] T. Xiao, Y. Liu, B. Zhou, Y. Jiang, J. Sun, Unified perceptual parsing for scene understanding, in: Proceedings of the European Conference on Computer Vision (ECCV), 2018, pp. 418–434.
- [47] M. Contributors, MMSegmentation: Openmmlab semantic segmentation toolbox and benchmark (2020).
- [48] H. Cai, J. Li, M. Hu, C. Gan, S. Han, Efficientvit: Lightweight multi-scale attention for high-resolution dense prediction, in: Proceedings of the IEEE/CVF Conference on Computer Vision and Pattern Recognition (CVPR), 2023, pp. 17302–17313.